

Effects of oleic acid and its congeners, elaidic and stearic acids, on the structural properties of phosphatidylethanolamine membranes

Sérgio S. Funari,^{1,2,*} Francisca Barceló,[†] and Pablo V. Escribá[†]

Max-Planck Institute for Colloids and Interfaces,* c/o HASYLAB, Notkestrasse 85, D-22603 Hamburg, Germany; and Molecular Cell Biology and Biochemistry,[†] Department of Biology, University of the Balearic Islands, E-07071 Palma de Mallorca, Spain

Abstract Fatty acid derivatives are abundant in biological membranes, mainly as components of phospholipids and cholesterol esters. Their presence, free or bound to phospholipids, modulates the lipid membrane behavior. The present study shows the differential influence of the C-18 fatty acids (FAs), oleic, elaidic, and stearic acids on the structural properties of phosphatidylethanolamine (PE). X-ray diffraction of PE-FA systems demonstrated that oleic acid (OA) produced important concentration-dependent alterations of the lipid membrane structure: it induced reductions of up to 20–23°C in the lamellar-to-hexagonal transition temperature of 1-palmitoyl-2-oleoyl PE and dielaidoyl PE and regulated the dimensions of the hexagonal lattice. In contrast, elaidic and stearic acids did not markedly alter the phospholipid mesomorphism. The above effects were attributed to the different “molecular shape” of OA (with a kink at the middle of the molecule) with respect to their congeners, elaidic and stearic acids. The effects of free fatty acids (FFAs) on membrane structure are relevant for several reasons: *i*) some biological membranes contain very high levels of FFAs. *ii*) Mediterranean diets with high OA intake have been shown to exert protective effects against tumoral and hypertensive pathologies. *iii*) FFA derivatives have been developed as antitumoral and antihypertensive drugs.—Funari, S. S., F. Barceló, and P. V. Escribá. Effects of oleic acid and its congeners, elaidic and stearic acids, on the structural properties of phosphatidylethanolamine membranes. *J. Lipid Res.* 2003. 44: 567–575.

Supplementary key words free fatty acids • phosphatidylcholine • lipid membrane structure • lamellar phases • nonlamellar phases • hexagonal H_{II} phase • epitaxial relationship

The lipid composition regulates the physicochemical properties of biological membranes, such as structure, fluidity/viscosity, permeability, microdomain formation, shear stress, etc. (1, 2). Lipid membrane properties regulate

membrane protein functions such as enzyme activity, protein-membrane interactions, receptor binding, etc. (3–8). In this context, fatty acids (FAs) are major components of membranes, mainly bound to phospholipids and cholesterol esters. In addition, free fatty acids (FFAs) can also be found in natural membranes. Their levels are usually low (around or under 1% of total lipids), but in certain membranes (such as the small intestine brush border membrane) they are important components whose abundance is similar to that of cholesterol or phosphatidylethanolamine (PE) (9). On the other hand, the composition of biological membranes is influenced by the type of fat present in the diet. Thus, diets rich in oleic acid (OA) (such as the Mediterranean diet) are associated with increased levels of this FA in various plasma membranes of rats and humans (10–12). Interestingly, changes in membrane levels of OA are accompanied by modulations in the function of various proteins (11, 12). Beyond the molecular and cellular considerations of the plasma membrane composition, it has been consistently observed that a high intake of OA is associated with a reduced risk of developing cardiovascular and tumoral pathologies (13–16). Moreover, synthetic derivatives of OA have been developed as anticancer and antihypertensive drugs because of the regulatory effects that they exert on membrane structure and signaling through G-protein-coupled receptors (Spain-Patent 200102269). However, the molecular mechanisms involved in the modulation of the membrane structure and function by FAs are not fully understood.

PE is the major phospholipid species in bacterial membranes and in the inner leaflet of mammalian plasma membranes (3). PE is mainly organized into lamellar structures that define the cell, constituting a physical boundary and support for the membrane proteins. PEs

Manuscript received 9 September 2002 and in revised form 10 December 2002.

Published, JLR Papers in Press, December 16, 2002.

DOI 10.1194/jlr.M200356.JLR200

¹ To whom correspondence should be addressed.
e-mail: sergio.funari@desy.de

² S. S. Funari and F. Barceló contributed equally to this work.

are hexagonal (H_{II})-prone lipids at high temperatures because of their “molecular shape,” which resembles a truncated cone and confers a negative curvature strain to model (17, 18) and biological membranes (19).

Numerous studies have demonstrated that localized or mobile, stable, or transient nonlamellar lipid structures exert defined membrane functions (4, 20, 21). Some of the roles attributed to H_{II} -prone phospholipids include facilitation of fusion and fission of bilayers (22, 23), modulation of membrane permeability and elasticity (2), protein transport (8), the regulation of G-protein and protein Kinase C (PKC) localization and activity (5–7), as well as chaperone-like activity (3) among others. Thus, the special features conferred to membranes by PE are crucial to membrane structure/function.

The present work was designed to study the effect of the C-18 FAs, OA (18:1 *cis* $\Delta 9$), elaidic acid (EA, 18:1 *trans* $\Delta 9$), and stearic acid (SA, 18:0) on the structural properties of lamellar and nonlamellar PE bilayers. In this context, X-ray scattering is the most appropriate technique to characterize the mesomorphic behavior of membrane phospholipids and the alterations induced by FAs or other molecules. Here, it has been shown that OA modulated the membrane structure, inducing negative membrane curvature strain (H_{II} -phase facilitation) on PE lipids, whereas the closely related FAs, EA and SA, did not alter markedly the phospholipid bilayer and H_{II} properties. Because the plasma membrane structure regulates a wide variety of cell functions (see above), the present results are relevant to understanding the relationship between membrane structure and function (e.g., 8, 24, 25).

EXPERIMENTAL PROCEDURES

Materials

1,2-dielaidoyl-*sn*-phosphatidylethanolamine (DEPE), 1,2-dioleoyl-*sn*-phosphatidylethanolamine (DOPE), and 1-palmitoyl,2-oleoyl-*sn*-phosphatidylethanolamine (POPE) were purchased from Avanti Polar Lipids, Inc. OA, EA, SA (18:0), and *N*-(2-hydroxyethyl) piperazine-*N'*-(2-ethanesulfonic acid) sodium salt (Hepes) were purchased from Sigma (Madrid, Spain). Lipid and FA stocks were stored under argon at -80°C until use. Control differential scanning calorimetry of multilamellar liposomes from these phosphatidylethanolamine (PE) derivatives were used to evaluate the phospholipid quality beyond TLC analysis. Calorimetric scans showed highly cooperative phase transitions at temperatures in agreement with published values (5).

Sample preparation

Multilamellar lipid vesicles (15% phospholipids; 85% water, by weight) were prepared in 20 mM Hepes, pH 7.4, in the absence or presence of the above FAs and at the molar ratio indicated below. Samples were thoroughly homogenized with a pestle-type minihomogenizer (Sigma) and vortexed until a homogeneous mixture was obtained. The suspensions were submitted to three temperature cycles (heated up to 70°C and cooled down to 4°C). Then, they were immediately stored at -80°C under argon until use. Before X-ray scattering experiments, samples were allowed to equilibrate at 4°C for 72 h.

X-ray scattering

Small- and wide-angle (SAXS and WAXS) synchrotron radiation X-ray scattering data were collected simultaneously using standard procedures on the Soft Condensed Matter beamline A2 (26–28) at the storage ring DORIS III of the Deutsches Elektronen Synchrotron (DESY).

Positions of the observed peaks were converted into distances, d , after calibration using standards with well-defined scattering patterns. Silver behenate and polyethylene terephthalate were used to calibrate the SAXS and WAXS regions, respectively. Data from each sample were acquired continuously for 15 s at each temperature, followed by a waiting time of 45 s with a local shutter closed. Linear detectors with delay line readout were used (29). The measurements were designed to compare the effects of the various FAs used on the H_{II} -phase propensity. During data collection, samples were heated from 27°C to 75°C (DEPE), 2°C to 32°C (DOPE), or 27°C to 80°C (POPE) at a scan rate of $1^{\circ}\text{C}/\text{min}$. Then, they were kept at the highest temperature for 5 min and finally cooled down to the lowest temperature at the same scan rate. At the end of the experiment, the samples were maintained at the lowest temperature for 5 min to confirm the phase structure. The experimental conditions did not affect the phase sequence structures or their parameters (e.g., their characteristic dimensions). Interplanar distances, d_{hkl} , were calculated according to Eq. 1:

$$s = 1/d_{hkl} = (2\sin\theta)/\lambda \quad (\text{Eq. 1})$$

where s is the scattering vector, 2θ is the scattering angle, λ (0.15 nm) is the X-ray wavelength, and hkl are the Miller indexes of the scattering planes. For H_{II} -phases, the unit-cell dimension, a , was calculated using the following relationship: $a = 2d_{10}/3^{1/2}$. This parameter (a) also corresponds to the diameter of the rods forming the hexagonal lattice.

The lamellar L_{α} phase was identified in the temperature scans by a single reflection peak at $s \sim 0.19 \text{ nm}^{-1}$, with a very good signal-to-noise ratio, occurring between patterns associated with the gel (L_{β}) and H_{II} phases.

RESULTS

DEPE systems

The structural properties of DEPE dispersions were analyzed in the absence or presence of increasing concentrations of OA, EA, and SA.

DEPE-OA mixtures. In the absence of OA, DEPE clearly showed a phase sequence from lamellar gel L_{β} to lamellar liquid crystalline L_{α} to hexagonal H_{II} phase, with increasing temperature. The presence of OA inhibited the occurrence of the L_{α} phase (Fig. 1). This effect was concentration dependent, since the range of temperatures where lamellar and nonlamellar phases occurred depended on the DEPE-OA molar ratio. The greater the OA content, the narrower the L_{α} -phase temperature range. At a molar ratio of 10:1, the L_{α} phase was not observed at all.

The incorporation of small amounts of OA into the DEPE bilayer increasingly induces the formation of H_{II} phase. At small amounts of OA, this phase has characteristics similar to the H_{II} phase formed by KH dioleate (30, and refs. therein) at higher water content, $\sim 42 \text{ wt}\%$. At high amounts of OA in the mixture, say PE-OA 1:1, one would expect a different effect, i.e., a separation of the

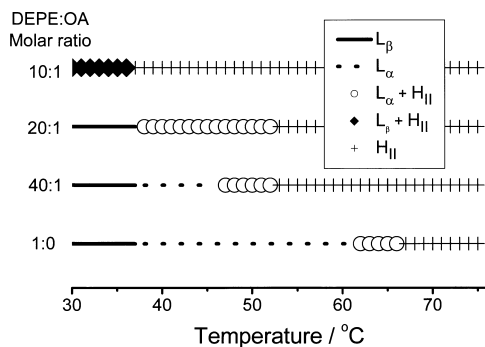


Fig. 1. 1,2-Dielaidoyl-*sn*-phosphatidylethanolamine (DEPE) and DEPE-oleic acid (OA) mesomorphism and phase transition temperatures. Increasing OA concentration induced reductions on the lamellar-to-hexagonal phase transition temperature, as determined by X-ray scattering. Signs corresponding to each lipid phase(s) are indicated in the inset.

mixture into two homogeneous phases: one, H_{II} , containing almost pure DEPE and another, L_{α} , containing almost only OA.

Lamellar phases. All samples studied showed a lamellar gel L_{β} phase up to 38°C with an approximately constant repeat distance of 6.4 nm. The similarity observed between gel phases of pure DEPE and DEPE-OA mixtures indicated a complete incorporation of the FA into the lipid bilayer, as previously described (31). DEPE, in the absence of FAs, showed a single L_{α} phase between 38–60°C. From 61°C to 66°C, L_{α} and H_{II} phases coexisted. Above 66°C DEPE was organized into an H_{II} structure. Along the temperature range L_{α} was observed, the repeat distance measured decreased linearly from 5.48 nm (38°C) to 5.11 nm (66°C). The lattice parameter for H_{II} phases also decreased linearly in a temperature-dependent manner. Compression coefficients for these structures are shown in **Table 1**.

The presence of OA drastically changed the temperature range of stability of the single L_{α} phase (Fig. 1). OA, at a molar ratio of 40:1 (DEPE-OA), induced a significant decrease (about 15°C) in the L_{α} -to- H_{II} phase transition temperature ($T_H = 46^\circ\text{C}$), and both phases coexisted in the range of 46°C to 52°C. Note the $\sim 6^\circ\text{C}$ temperature range of coexistence of these phases, as observed in the single DEPE system. The L_{β} -to- L_{α} transition, however, was not markedly altered by the presence of the FA ($T_m = 37^\circ\text{C}$ in the absence or presence of OA). The influence of OA was further evidenced by the enhancement of the thermal sensitivity of the lamellar lattice parameter ($\partial d/\partial T$), whose value changed from $-0.012\text{nm}/^\circ\text{C}$ (in the absence of OA) to $-0.016\text{nm}/^\circ\text{C}$ (in the presence of OA). Higher OA content (DEPE-OA 20:1, mol/mol) (**Figs. 2, 3**) induced greater effects on the structural properties of DEPE dispersions. First, the occurrence was observed of a broad peak alongside the reflections characteristic of the gel L_{β} phase. Heating induced a shift of this broad peak toward smaller angles, accompanied by a loss in resolution. Further characterization of this peak was not possible with the available data. Second, the L_{β} phase was clearly identified by a sharp and intense SAXS reflection, accompanied by a

TABLE 1. Sample composition and their physical (structural) characteristics

Composition	Molar Ratio	$\partial d/\partial T$ for L_{α}^a	$\partial d/\partial T$ for H_{II}^a	$\Delta T_{L_{\alpha}}/^\circ\text{C}^b$	$d_{H_{II}}/\text{nm}$
DEPE	ND	-0.012	-0.024	38–61 (66)	Values at 72°C 6.27
DEPE-OA	40:1	-0.016	-0.023	37–46 (52)	6.09
DEPE-OA	20:1	-0.014	-0.024	(39)–(53) ^c	5.87
DEPE-OA	10:1	ND	-0.020	ND	5.21
DEPE-SA	20:1	-0.013	-0.022	39–60 (66)	6.33
DEPE-EA	20:1	-0.013	-0.022	38–57 (59)	6.21
DEPE-EA	10:1	-0.012	-0.023	38–54 (58)	6.15
					Values at 30°C
DOPE ^d	ND	ND	-0.021	ND	6.28
DOPE-OA ^d	20:1	ND	-0.014	ND	5.47
DOPE-EA ^d	20:1	ND	-0.022	ND	6.09
					Values at 72°C
POPE	ND	-0.010	-0.029	(<30)37–71(>80)	6.34 ^e
POPE/OA	10:1	-0.011	-0.019	35–51 (62)	5.92

DEPE, 1,2-dielaidoyl-*sn*-phosphatidylethanolamine; DOPE, 1,2-dioleoyl-*sn*-phosphatidylethanolamine; EA, elaidic acid; OA, oleic acid; POPE, 1-palmitoyl,2-oleoyl-*sn*-phosphatidylethanolamine. The angular coefficient of the dependence of the interplanar distance d_{10} on the temperature $\partial d/\partial T < 0$ indicates a compression process. The temperature range where the L_{α} phase is observed is shown in $\Delta T_{L_{\alpha}}$.

^a The compressibility of L_{α} and H_{II} phases are linear, both in single- or two-phase regions.

^b The parentheses indicate the temperature limit of the L_{α} phase in a two-phase region. Values on the left correspond to $L_{\beta}+L_{\alpha}$, and on the right to $L_{\alpha}+H_{II}$ temperature range.

^c Measured from 32°C to 2°C. Only a hexagonal H_{II} phase was observed.

^d No single L_{α} phase was observed. Up to 45°C, $L_{\beta}+L_{\alpha}$ are seen together, and above that temperature, $L_{\alpha}+H_{II}$ phases coexisted.

^e Measured in the $L_{\alpha}+H_{II}$ phase region.

well-defined reflection in the WAXS region (Fig. 2). The corresponding lamellar spacing remained constant in the temperature range of its occurrence.

OA strongly destabilized DEPE lamellar L_{α} phase, which was observed only from 38°C to 53°C and coexisted with either L_{β} or H_{II} phases (DEPE-OA, 20:1 mol/mol). The thermal sensitivity of the lamellar lattice parameter ($\partial d/\partial T$) was $-0.014\text{nm}/^\circ\text{C}$. An interesting aspect of this transition was the continuity of the interplanar distance between L_{β} and H_{II} phases, which led us to consider an epitaxial relationship between the (10)-planes of both phases (see below). In this situation, the phase transition was identified by the WAXS region peaks (Fig. 2). The complete vanishing of the peak in the WAXS characterized the change from a well-organized all-trans to liquid-like conformation of the acyl chains of the phospholipid and OA present in the mixture. It is also interesting to note that in the temperature range where L_{α} and H_{II} phases coexisted, the lattice parameter of the hexagonal phase H_{II} remained basically constant (6.4 nm), decreasing only after the system turned monophasic (Fig. 3).

In the presence of higher OA concentrations (DEPE-OA, 10:1, mol/mol), the L_{α} phase was not observed over the temperature range studied (27–75°C) (**Figs. 4, 5**). The L_{β} phase appeared between 27°C and 35°C, coexisting

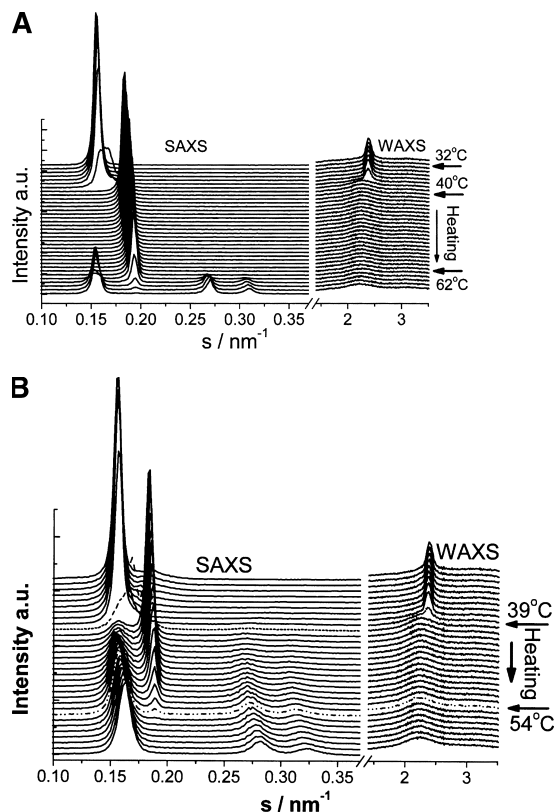


Fig. 2. Heating sequence of X-ray scattering patterns of (A) DEPE and (B) DEPE-OA (20:1, mol/mol). Heating and cooling scan rates were 1°C/min from 27°C to 75°C. Successive diffraction patterns were collected for 15 s every min. Thermal sequence of phases from L_{β} to L_{α} to H_{II} is clearly observed. Note the apparent epitaxial relationship between the L_{β} and H_{II} phases, with SAXS peaks in the same position (B) but different profile as the transition takes place. In addition, the order-disorder phase transition from L_{β} to H_{II} could be identified by the vanishing peak on the WAXS region of the pattern.

with the hexagonal phase. Above this temperature, the L_{β} phase vanished and the lipids reorganized directly into H_{II} phase (35–75°C) without transit through the liquid crystalline L_{α} phase. It is noteworthy that the L_{β} phase showed also a constant lattice parameter of 6.35 nm along the temperature range where it was observed, but the H_{II} showed a different behavior (Fig. 3). In the two-phase temperature range (27–35°C), H_{II} phases expanded linearly ($\partial d/\partial T = 0.13$ nm/°C), whereas in the single phase region, there was a temperature-dependent contraction ($\partial d/\partial T = -0.020$ nm/°C). In addition, this phase contraction was one order of magnitude smaller than the H_{II} phase expansion observed in the two-phase region.

H_{II} phases. In all DEPE-OA mixtures studied, a single hexagonal phase appeared at high temperatures (Figs. 3, 5). At lower temperatures, lamellar (L_{α} or L_{β}) and H_{II} structures coexisted. The threshold temperature for H_{II} phases, either alone or forming a binary system, greatly depended on OA concentration. For low OA concentrations (DEPE-OA, 40:1 and 20:1, mol/mol), the binary system consisted of H_{II} and lamellar L_{α} phases, while for high OA concentrations (DEPE-OA, 10:1, mol/mol), the

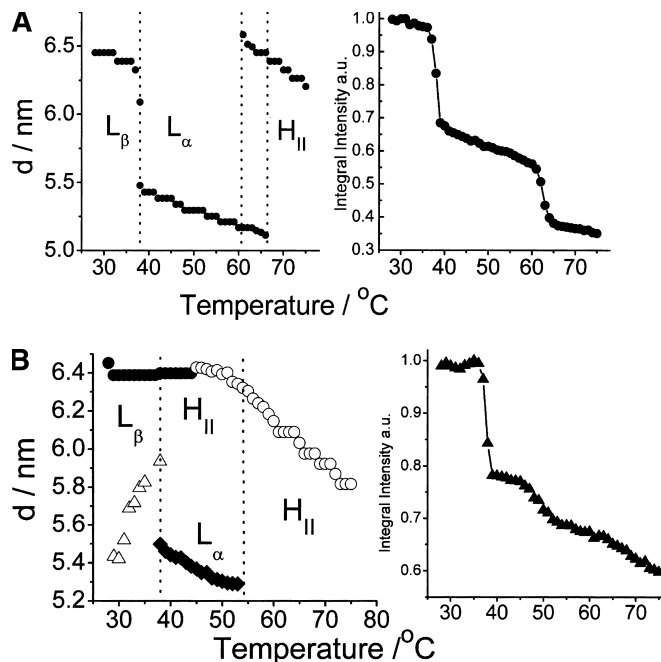


Fig. 3. Dependence of the interplanar repeat distance d with temperature for (A) DEPE, (B) DEPE-OA (20:1, mol/mol). Phases represented are: (closed circle) L_{β} , (triangle) unidentified phase seen as broad and very weak peaks at $s \sim 0.18$ nm $^{-1}$ during the heating scan, (diamond) L_{α} , and (open circle) H_{II} . Note the apparent continuity of the parameter d between L_{β} and H_{II} phases in B.

binary system was formed by H_{II} and L_{β} structures. The temperature range of coexistence of these phases also depended on the DEPE-OA ratio in the mixture. For all DEPE-OA systems studied, the compressibility of the H_{II} lattice parameter was inversely proportional to temperature increase ($\partial d/\partial T \cong -0.022$ nm/°C). The H_{II} phase contraction factor was about 2-fold greater than that of the lamellar L_{α} phase ($\partial d/\partial T \cong -0.014$ nm/°C) (Table 1). This effect is indicative of a phase dehydration with a concomitant reduction of the surface area per molecule. The negative value of the thermal coefficient ($\partial d/\partial T < 0$) for both phases (L_{α} and H_{II}) can be attributed to a continuous coiling up of the acyl chains forming the mesomorphic units of the structures. At the initial formation of the hexagonal phase, a typical lattice spacing of 6.4 nm was observed, with the exception of DEPE-OA at a molar ratio of 10:1 for which this value was smaller (i.e., 5.9 nm). This reduced value of the lattice parameter implies a more effective packing of the molecules, and may account for the direct transition between L_{β} and H_{II} phases, without the formation of the liquid crystalline lamellar L_{α} phase.

“Apparent” epitaxial relationship. Structural aspects of the L_{β} -to- H_{II} phase transition of DEPE-OA (20:1, mol/mol) are complex. The sequence of diffraction patterns collected during the temperature scans showed defined phase transitions that allowed unequivocal characterization of the structures and their respective lattice parameters. The diffraction patterns always showed a peak at $s = 0.155$ nm $^{-1}$ (see Eq. 1 in Experimental Procedures), which apparently related epitaxially the L_{β} and H_{II} phases. Al-

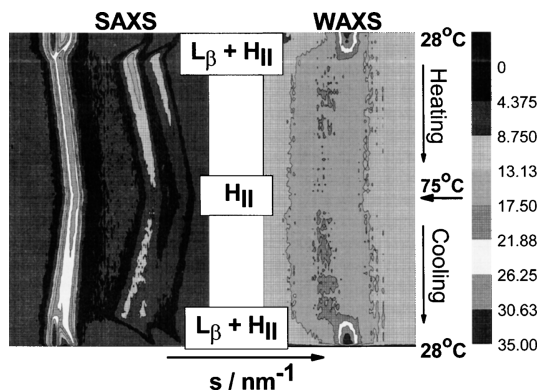


Fig. 4. Contour plot of SAXS (left) and WAXS (right) scattering patterns of DEPE-OA (10:1, mol/mol). Note the absence of the L_{α} phase and the different thermal behavior of the H_{II} phase, expanding in the $L_{\beta} + H_{II}$ (two-phase) region and compressing in the single-phase region.

though through the transition the broadness and intensity of this peak changed drastically, its position could still be clearly identified. It was associated with the (10)-planes of both L_{α} and H_{II} phases. Changes in the peak features marked the L_{β} -to- H_{II} phase transition, where significant morphological changes in the mesogenic units take place; therefore, neither positional nor orientational order can be maintained properly, causing the peak broadening. Simultaneously, the phase transition was also observed between L_{β} and L_{α} phases, with onset at the same temperature. In this situation, the gel phase initially develops into two phases, L_{α} and H_{II} phases. At higher temperatures, L_{α} also turns into a H_{II} phase. The mechanism of such complex phase transition is still unclear and beyond the scope of the present study. With the data available, we could not quantify the relative amount of each phase formed upon the gel transition. However, the peak intensities ($s = 0.155 \text{ nm}^{-1}$) suggested a greater abundance of L_{α} phase with re-

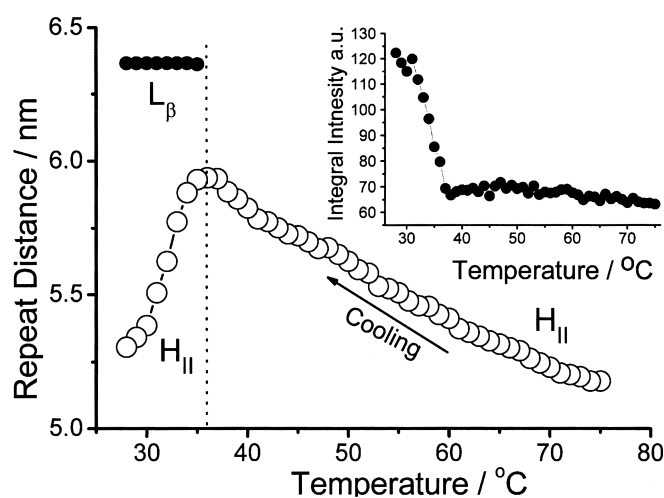


Fig. 5. Dependence of the interplanar repeat distance d of DEPE-OA (10:1, mol/mol) upon cooling. Phases are represented by: (closed circle) L_{β} and (open circle) H_{II} . No L_{α} phase was observed. The H_{II} phase expands in the $L_{\beta} + H_{II}$ two-phase region and contracts in the single-phase region.

spect to H_{II} phases when both phases coexisted in the DEPE-OA sample at a molar ratio of 20:1. This could be due to the melting of the acyl moiety that induced a negative curvature strain necessary to form rods characteristic of hexagonal phases. In this system, the lamellar phase plays the role of an intermediate, as in chemical reactions, in which the transformation among reagents and products follows a competitive path between kinetic and energetic dominance. For the DEPE-OA (20:1) system, the L_{α} phase is kinetically favorable but with higher total energy, therefore soon after its formation, it transforms into the energetically favorable hexagonal phase. Although the phase transition contained the elements required for an epitaxial relationship between these phases, additional events taking place simultaneously, e.g., the formation of the L_{α} phase, impaired a proper classification as such. Therefore, we called it an “apparent” epitaxial relationship between gel and H_{II} phases.

Although little is known about the modulation of membrane structural properties by FAs, there is evidence that the incorporation of amphiphilic molecules into the lipid matrix induces drastic changes in the bilayer behavior. For example, the addition of nonionic surfactants into phosphatidylcholine bilayers modifies the structure of the lipid self-assembly when compared with the phospholipid alone (32). Thus, in the presence of $C_{12}EO_4$ (tetraethyleneglycol-mono-*n*-dodecylether), dipalmitoyl phosphatidylcholine (a lamellar-prone lipid) formed a pseudobinary mixture in excess of water (33). Similarly, POPC organizes into H_{II} phases in the presence of $C_{12}EO_2$, although neither molecule aggregates into nonlamellar structures separately (34). $C_{12}EO_2$ -POPC (1:2, mol/mol) mixtures are arranged into L_{β} and H_{II} structures below 20°C , but only a single H_{II} phase is observed above this temperature. Interestingly, in the two-phase region, the H_{II} phase expands while heating, but when the system turns into a single H_{II} phase, it undergoes contraction (35). A similar behavior was observed here for DEPE-OA, 10:1 (mol/mol).

Recently, Yang and Huang, studying diphytanoyl phosphatidylcholine (DPhPC) supported on a silicon nitride window using 2D diffraction patterns, were able to determine the structure of a stalk (rhombohedral), an intermediate structure between L_{α} and H_{II} (36). This structure is part of a current model for cell fusion, thus the strong interest in determining its parameters and conditions of occurrence. The spontaneous question that arises is if we would get the same structure using similar preparations and conditions with our samples. We do not expect so for different reasons. First, our samples contain much more water, 85 wt%, which brings the system to an excess of water condition. This means both lipid and FA in the mixture are fully hydrated, against a relative humidity of 70–80% in the study on DPhPC. Finally, in multi-component systems, one would expect that at a point of large changes in topology, as is necessary for the formation of the stalk structure, segregation between the components should occur. In this situation, the system can no longer be considered homogeneous on a microscale; therefore, comparison between these systems has to be viewed with great

care and attention to their differences in preparation. Moreover, the system based on the polyoxyethylene glycol-alkyl ether, C₁₆EO₆, in water when studied under very slow temperature scan rate, also showed a rhombohedral phase (37), but with no indication of stalk formation, although the X-ray data were collected with a linear detector. Despite large differences in structure, C₁₆EO₆ and DPhPC have in common a similar chain length and a large uncharged head group different from our samples.

DEPE-EA and DEPE-SA mixtures. EA and SA are FAs closely related to OA in terms of chemical structure (SA is a saturated 18:0 FA and EA is an isomer of OA, both 18:1 FAs). Conversely to OA, its congeners EA and SA induce smaller changes in the structural properties of DEPE. The mixtures DEPE-EA (20:1 and 10:1, mol/mol) and DEPE-SA (20:1, mol/mol) (Table 1, Fig. 6) followed a similar trend. In DEPE-SA mixtures, L_α was observed as a single phase up to 60°C, and it was present until 66°C along with an H_{II} phase. In the absence of SA, the temperatures for these phases were 61°C and 66°C, respectively. DEPE-EA (20:1, mol/mol) mixtures showed a single L_α phase up to 57°C and L_α+H_{II} up to 59°C. Over 66°C for DEPE-SA, and over 59°C for DEPE-EA, a single H_{II} phase was observed (Table 1). On the other hand, the H_{II} lattice parameter of DEPE was altered by OA (6.27 nm and 5.87 nm for DEPE and DEPE-OA, 20:1, mol/mol, respectively), but EA and SA did not induce important changes in this parameter at 72°C (6.21 nm and 6.33 nm, respectively) (Table 1).

DOPE systems

DOPE arranges into nonlamellar H_{II} structures at low (physiological) temperatures. Using this lipid, we could study the influence of the FA conformation (*cis* or *trans*) on the hexagonal phase properties between 2°C and 32°C (Table 1). In these phospholipid-FA mixtures, EA had little effect on DOPE structures compared with its *cis* isomer, OA. Differences in *d*₁₀ values at 30°C support the specific effect of the *cis* double bond conformation on the phospholipid structure dimensions. The mixture of DOPE-OA had a significantly smaller lattice value (*d*₁₀ = 5.47 nm), and therefore a smaller rod diameter than DOPE-EA (*d*₁₀ = 6.09 nm) and pure DOPE (*d*₁₀ = 6.28 nm). The thermal

compression of the hexagonal lattice parameter ($\frac{\partial d}{\partial T} \sim -0.021 \text{ nm}/^\circ\text{C}$) for DOPE and DOPE-EA was similar to that of DEPE samples. In contrast, the mixture DOPE-OA had a significantly different value ($\frac{\partial d}{\partial T} \sim -0.014 \text{ nm}/^\circ\text{C}$), indicating that the thermal sensitivity of DOPE is altered by the presence of OA. Comparison of the systems DOPE-OA and DEPE-OA at the same molar ratio (20:1) also demonstrated the influence of the *cis* double bond on the phospholipid structure, inducing the formation of H_{II} phase in mixtures containing DOPE, but not DEPE at 30°C (Table 1).

POPE systems

We also studied the effect of OA on POPE to further determine the effect of this FA on another PE derivative with two different acyl chains. POPE dispersions organized into lamellar phases over most of the temperature range studied (27°C to 80°C). L_β and L_α phases coexisted and could be individually identified over a large range of temperatures up to 37°C. Between 37°C to 71°C, we observed a single lamellar (L_α) phase. Over 71°C, L_α and H_{II} phases coexisted. In the temperature range of this study, a single-H_{II} phase was not observed. OA lowered the L_α-to-H_{II} phase transition temperature from 71°C to 51°C. Above 51°C, both L_α and H_{II} phases coexisted up to 62°C when the system turned into a single H_{II} phase (Fig. 7). This result clearly indicated that OA also facilitated the formation of POPE hexagonal phases. The lattice parameter of POPE was also altered by the presence of OA (6.34 nm and 5.92 nm in the absence or presence of OA, respectively). The compressibility factor for the H_{II} phase of POPE ($-0.029 \text{ nm}/^\circ\text{C}$) increased in the presence of OA ($-0.019 \text{ nm}/^\circ\text{C}$), similar to what it was observed for DEPE and DOPE. It should be noted that for phospholipid-OA mixtures with molar ratio 10:1, DEPE and POPE showed essentially the same compressibility factor (Table 1).

DISCUSSION

FAs are important components of plasma and other membranes. The membrane core is formed by the FA

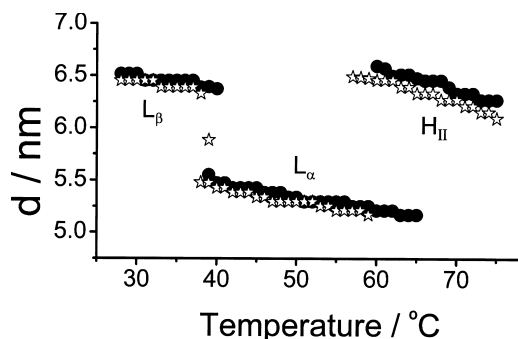


Fig. 6. Dependence of interplanar repeat distance *d* of (circle) DEPE-SA and (open stars) DEPE-elaidic acid (EA) (20:1, mol/mol) upon heating mixtures. The effect of these fatty acids (FAs) is very small and similar.

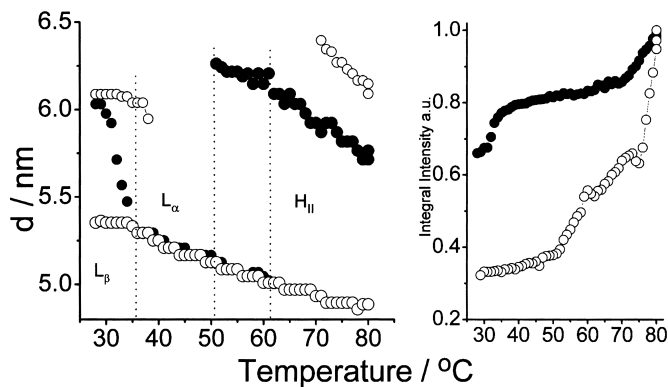


Fig. 7. Dependence of interplanar repeat distance *d* of (open circle) 1-palmitoyl,2-oleoyl-*sn*-phosphatidylethanolamine (POPE), and (closed circle) POPE-OA (10:1, mol/mol) upon cooling mixtures. Note that the H_{II} phase contracts linearly.

moieties of phospholipid and cholesterol esters. In addition, low levels of FFAs are also present in biological membranes (9, 38) (around 0.3–10% of total lipids) whereas PE constitutes about 5–50% of total lipids in membranes, so that the FA-PE ratios used here are of biological relevance. In this context, it is of special interest to study the effects of FAs on membrane structure because of its further influence on membrane protein function. Several works support the involvement of the plasma membrane properties in the control of membrane protein activity and the cell physiology (1, 39–41). Moreover, altered levels of FFAs have been associated with pathological states (38). In addition, the relevance of FAs in the control of the membrane structure and function is noteworthy in small intestine brush border membranes, which contain high levels of FFAs (comparable to the levels of cholesterol and the major phospholipid species) (9). These membranes are specialized in internalizing nutrients from the intestine lumen, so that transport and exoendocytic processes are common events in this type of membrane. These cellular functions are facilitated by the hexagonal-phase propensity (42), which is highly favored by the presence of OA, as it is shown in our study. Then, the results shown here may explain, at least in part, the role of FAs in the special properties of brush border membranes or during certain pathological states. On the other hand, the type of fat in the diet modulates the levels of FAs in cell membranes (10–12, 43). The Mediterranean diet is rich in olive oil, mainly composed by triglycerides (containing about 80% of OA), which are processed by lipases and other enzymes during digestion. High olive oil intake has been associated with a lesser incidence of hypertension and cancer (14, 16, 44–46). Until now, the healthy effects of olive oil have not been associated with any specific mechanism of action. The present study constitutes a first step to understanding the possible relationship between OA/olive oil intake and its cardiovascular and antitumoral effects: olive oil intake increases the levels of OA, which can modulate the membrane structure with a concomitant regulation in the localization and/or activity of signaling proteins (G-proteins, PKC, and adenylyl cyclase) (5). Regulation of adenylyl cyclase activity controls blood pressure (47), in agreement with the hypotensive effects of OA derivatives (Spain-Patent 200102269).


H_{II}-prone phospholipids, such as PE, are involved in a number of cellular functions, including the development of endocytic (membrane fission) and exocytic (membrane fusion) processes (42) and the regulation of activities of membrane proteins (2, 48). PE has been shown to accumulate at the cleavage furrow during cell division in *E. coli* (23) and exhibits a chaperone-like activity in *E. coli* (3). The high proportion of PE in membranes and the precise regulation of their levels indicate that this lipid has a great functional relevance (49). Because PE is a major membrane lipid species capable of organizing into nonlamellar phases, and the FA composition modulates the membrane properties, this work was designed to study the effects of OA (and its congeners EA and SA) on membrane mesomorphism. In this context, the FA concentra-

tion and the conformation of its double bond appeared to be important factors that influenced the properties of macrostructures formed by the mixtures used in this study. Thus, OA induced important concentration-dependent alterations in the supramolecular organization of PE derivatives, whereas the closely related FAs, EA and SA, did not. OA probably exerted a lateral pressure on PE FA moieties, favoring a negative-curvature strain. This effect induced the formation of inverted tubular micelles, which are the basic supramolecular units of the H_{II}-phase lattice. This hypothesis is consistent with the marked decrease of the L_α-to-H_{II} phase transition temperature induced by OA. In contrast, EA and SA exerted very modest effects on PE structural properties. The different effects promoted by OA, EA, and SA on lipid mesomorphism could be also explained from the point of view of the lipid packing parameter (50). This property has been used to explain secondary structures formed by membrane lipids (51). Thus, lamellar phases are favored by cylinder-shaped phospholipids (e.g., PC with a bulky polar head), and inverted micelles, such as H_{II} phases, are formed by truncated cone-shaped phospholipids (e.g., PE with a small polar head). With respect to the FA structure, OA (18:1 *cis* Δ9) has a “molecular shape” similar to a boomerang, whereas EA (18:1 *trans* Δ9) and SA (18:0) resemble a rod. This is the main structural difference between OA and its congeners EA and SA. In fact, the chemical compositions of OA and EA are identical (C₁₈O₂H₃₄), while SA (C₁₈O₂H₃₆) has only 2 H more because of the absence of double bonds. The effect of OA cannot be only attributed to the presence of a double bond, since EA did not exert similar effects on PE structure. Moreover, EA and SA, which differ in chemical composition but are closer in terms of “molecular shape,” appeared to have similar (modest) effects on the membrane structure. Then, OA effects on PE lipid mesomorphism are most probably due to its molecular structure. Epand et al. (31) observed an enhanced ability of OA, with respect to other FAs, for lowering the bilayer-to-hexagonal phase temperature at different pHs. Our hypothesis, based on the FA “molecular shape,” also explains the ability of OA to facilitate nonlamellar phases from a complementary point of view. Moreover, the present study identifies each phase coexisting in multi-phase regions, whose extent is dependent not only on the FA conformation but also on its concentration.

The thermal compressibility factor of the different phases also evidenced differences between OA, EA, and SA on the behavior of PE macrostructures. The compressibility of the L_α-lattice parameter ($\partial d/\partial T \cong -0.013 \text{ nm}/^\circ\text{C}$) was similar for all DEPE samples studied. For DEPE H_{II} phases, the thermal compressibility factor was about $-0.022 \text{ nm}/^\circ\text{C}$. However, the presence of OA in DOPE membranes (DOPE-OA, 20:1, mol/mol) induced a marked alteration of this parameter ($\partial d/\partial T = -0.014 \text{ nm}/^\circ\text{C}$). Conversely, EA did not induce any decrease in the DOPE lattice thermal compressibility factor ($\partial d/\partial T \cong -0.022 \text{ nm}/^\circ\text{C}$). These results highlight, on one hand, the influence of OA on nonlamellar membrane structures, and suggest cooperative effects between OA (FFA) and the FA moi-

eties (also OA residues) of DOPE. A direct effect of this cooperativity is an improved packing of DOPE molecules in the H_{II} structure.

EA and SA had little effect on the L_α-to-H_{II} DEPE phase transition temperature ($\Delta T = -4$ and -1°C , respectively) at a molar ratio 20:1 (DEPE-FA). In contrast, OA induced very important alterations of this temperature ($\Delta T = -16^\circ\text{C}$) at the same molar ratio (Table 1, Fig. 1). As a matter of fact, for the DEPE-OA mixture at a molar ratio of 20:1, L_α phase was not observed as a single phase and at a molar ratio of 10:1 was not observed at all. Similarly, the POPE-OA mixture (10:1, mol/mol) showed a decrease in the L_α-to-H_{II} phase transition of about 20°C, albeit here L_α phases appeared over a narrow temperature range, indicating that the effect of OA depended also on the FA moieties species of the PEs.

In summary, the present work quantifies the effects of the FAs OA, EA, and SA on membrane structure. From the structural behavior of the model systems studied here, we conclude that the FA molecular shape facilitates the H_{II} phase formation by modulating the bilayer curvature. This regulation of the membrane structure explains in part the modulation exerted by OA on membrane and cell functions: membrane fluidity, permeability, domain formation, exo/endocytosis, cell division, signal transduction, membrane protein (G-proteins, G-protein-coupled receptors, adenylyl cyclase) activities, blood pressure control, and antiproliferative (antitumoral) effects. 

The authors thank Andreas Meyer and Ralph Döhrmann for their invaluable support during the measurements, and Frank Richter for support with data processing and figures. This work was supported in part by grants FIS 00/1029, PETRI 95-0421, and SAF2001-0839 from the Ministerio de Sanidad y Consumo and Ministerio de Ciencia y Tecnología (Spain), and by project I-01-100EC from Deutsches Elektronen-Synchrotron DESY (Hamburg-Germany).

REFERENCES

1. Hampton, M. J., R. A. Floyd, J. B. Clark, and J. H. Lancaster. 1980. Studies of the fatty acid composition and membrane microviscosity in *Salmonella typhimurium* TA98. *Chem. Phys. Lipids*. **27**: 177–183.
2. Gudi, S., J. P. Nolan, and J. A. Frangos. 1998. Modulation of GTPase activity of G proteins by fluid shear stress and phospholipid composition. *Proc. Natl. Acad. Sci. USA*. **95**: 2515–2519.
3. Bogdanov, M., J. Sun, H. R. Kaback, and W. Dowhan. 1996. A phospholipid acts as a chaperone in assembly of a membrane transport protein. *J. Biol. Chem.* **271**: 11615–11618.
4. de Kruijff, B. 1997. Biomembranes. Lipids beyond the bilayer. *Nature*. **386**: 129–130.
5. Escribá, P. V., M. Sastre, and J. A. García-Sevilla. 1995. Disruption of cellular signaling pathways by daunomycin through destabilization of nonlamellar membrane structures. *Proc. Natl. Acad. Sci. USA*. **92**: 7595–7599.
6. Escribá, P. V., A. Ozaita, C. Ribas, A. Miralles, E. Fodor, T. Farkas, and J. A. García-Sevilla. 1997. Role of lipid polymorphism in G protein-membrane interactions: Nonlamellar-prone phospholipids and peripheral protein binding to membranes. *Proc. Natl. Acad. Sci. USA*. **94**: 11375–11380.
7. Giorgione, J., R. M. Eppard, C. Buda, and T. Farkas. 1995. Role of phospholipids containing docosahexaenoyl chains in modulating the activity of protein kinase C. *Proc. Natl. Acad. Sci. USA*. **92**: 9767–9770.
8. Rietveld, A. G., M. C. Koorengel, and B. de Kruijff. 1995. Non-bilayer lipids are required for efficient protein transport across the plasma membrane of *Escherichia Coli*. *EMBO J*. **14**: 5506–5513.
9. Hauser, H., K. Howell, R. M. Dawson, and D. E. Bowyer. 1980. Rabbit small intestinal brush border membrane preparation and lipid composition. *Biochim. Biophys. Acta*. **602**: 567–577.
10. Escudero, A., J. C. Montilla, J. M. García, M. C. Sánchez-Quevedo, J. L. Periago, P. Hortelano, and M. D. Suárez. 1998. Effect of dietary (n-9), (n-6) and (n-3) FAs on membrane lipid composition and morphology of rat erythrocytes. *Biochim. Biophys. Acta*. **1394**: 65–73.
11. Pagnan, A., R. Corocher, G. B. Ambrosio, S. Ferrari, P. Guarini, D. Piccolo, A. Opportuno, A. Bassi, O. Olivieri, and G. Baggio. 1989. Effects of an olive-oil-rich diet on erythrocyte membrane lipid composition and cation transport systems. *Clin. Sci*. **76**: 87–93.
12. Vicario, I. M., D. Malkova, E. K. Lund, and I. T. Johnson. 1998. Olive oil supplementation in healthy adults: effects in cell membrane FA composition and platelet function. *Ann. Nutr. Metab*. **42**: 160–169.
13. Dominiczak, A. F., Y. McLaren, J. R. Kusel, D. L. Ball, T. L. Goodfriend, D. F. Bohr, and J. L. Reid. 1993. Lateral diffusion and FA composition in vascular membrane from stroke-prone spontaneously hypertensive rats. *Am. J. Hypertens*. **6**: 1003–1008.
14. Ruiz-Gutiérrez, V., F. J. Muriana, A. Guerrero, A. M. Cert, and J. Villar. 1996. Plasma lipids, erythrocyte membrane lipids and blood pressure of hypertensive women after ingestion of dietary oleic acid from two different sources. *J. Hypertens*. **14**: 1483–1490.
15. Martín-Moreno, J. M., W. C. Willett, L. Gorgojo, J. R. Banegas, F. Rodríguez-Artalejo, J. C. Fernández-Rodríguez, P. Maisonneuve, and P. Boyle. 1994. Dietary fat, olive oil intake and breast cancer risk. *Int. J. Cancer*. **58**: 774–780.
16. Tzonou, A., L. Lipworth, A. Kalandidi, A. Trichopoulou, I. Gamsati, C.-C. Hsieh, V. Notara, and D. Trichopoulos. 1996. Dietary factors and the risk of endometrial cancer: A case-control study in Greece. *Br. J. Cancer*. **73**: 1284–1290.
17. Seddon, J. 1990. Structure of the inverted hexagonal (H_{II}) phase and non-lamellar phase transitions of lipids. *Biochim. Biophys. Acta*. **1031**: 1–69.
18. Turner, D. C., and S. M. Gruner. 1992. X-ray diffraction reconstruction of the inverted hexagonal (H_{II}) Phase in lipid-water systems. *Biochemistry*. **31**: 1340–1355.
19. Borovoyagin, V. L., and A. G. Sabelnikov. 1989. Lipid polymorphism of model and cellular membranes as revealed by electron microscopy. *Electron Microsc. Rev.* **2**: 75–115.
20. Siegel, D. P. 1986. Inverted micellar intermediates and transitions between lamellar, cubic and inverted hexagonal lipid phases. Implications for membrane-membrane interactions and membrane fusion. *Biophys. J.* **49**: 1171–1183.
21. Lindblom, G., and L. Rilfors. 1990. Structures formed by membrane lipids-physicochemical properties and possible biological relevance for membrane function. In *Dynamics and biogenesis of membrane*. J. A. F. Op den Kamp, editor. Vol. H 40. PA.NATO ASI Series, Springer-Verlag, Berlin and Heidelberg. 43–64.
22. Siegel, D. P., J. Banschbach, D. Alford, H. Ellens, L. J. Lis, P. J. Quinn, L. Yeagle, and J. Bentz. 1989. Physiological levels of diacylglycerols in phospholipid membranes induce membrane fusion and stabilize inverted phases. *Biochem. J.* **28**: 3703–3709.
23. Emoto, K., T. Kobayashi, A. Yamaji, H. Aizawa, I. Yahara, K. Inoue, and M. Umeda. 1996. Redistribution of phosphatidylethanolamine at the cleavage furrow of dividing cells during cytokinesis. *Proc. Natl. Acad. Sci. USA*. **93**: 12867–12872.
24. Soulages, J. L., Z. Salamon, M. A. Wells, and G. Tollin. 1995. Low concentrations of diacylglycerol promote the binding of apolipoprotein III to a phospholipid bilayer: A surface plasmon resonance spectroscopy study. *Proc. Natl. Acad. Sci. USA*. **92**: 5650–5654.
25. Starling, A. P., K. A. Dalton, J. M. East, S. Oliver, and A. G. Lee. 1996. Effects of phosphatidylethanolamines on the activity of the Ca²⁺-ATPase of sarcoplasmic reticulum. *Biochem. J.* **320**: 309–314.
26. Koch, M. H. J., and J. Bordsas. 1983. X-ray diffraction and scattering on disordered systems using synchrotron radiation. *Nucl. Instrum. Methods Phys. Res.* **208**: 461–469.
27. Boulin, C., R. Kempf, M. H. J. Koch, and S. M. McLaughlin. 1986. Data appraisal, evaluation and display for synchrotron radiation experiments: hardware and software. *Nucl. Instrum. Methods Phys. Res.* **A249**: 399–407.

28. Boulin, C., R. Kempf, A. Gabriel, and M. H. J. Koch. 1988. Data acquisition systems for linear and area X-ray detectors using delay line readout. *Nucl. Instrum. Methods Phys. Res.* **A269**: 312–320.
29. Gabriel, A., and F. Dauvergne. 1982. The localization method used at EMBL. *Nucl. Instrum. Methods Phys. Res.* **201**: 223–224.
30. Cistola, D. P., J. A. Hamilton, D. Jackson, and D. M. Small. 1988. Ionization and phase behaviour of fatty acids in water: Application of the Gibbs phase rule. *Biochemistry*. **27**: 1881–1888 (and refs. therein.).
31. Epand, R. M., R. F. Epand, N. Nadeem, and R. Chen. 1991. Promotion of hexagonal phase formation and lipid mixing by fatty acids with varying degrees of unsaturation. *Chem. Phys. Lipids*. **57**: 78–80.
32. Rapp, G., S. S. Funari, F. Richter, and D. Woo. 2000. X-ray diffraction studies on the effect of additives on the phase behaviour of lipids. In *Lipid Bilayers. Structure and Interactions*. J. Katsaras, and T. Gutberlet, editors. Springer, Heidelberg. 165–188.
33. Madler, B., G. Klose, A. Mops, W. Richter, and C. Tschierske. 1994. Thermotropic phase behaviour of the pseudobinary mixture DPPC/C₁₂E₄ at excess water. *Chem. Phys. Lipids*. **71**: 1–12.
34. Funari, S. S. 1998. Induction of a hexagonal phase in phospholipid-surfactant bilayers. *Eur. Biophys. J.* **27**: 590–594.
35. Funari, S. S., C. di Vita, and G. Rapp. 1997. X-ray Diffraction and NMR Studies on mixtures of non-ionic surfactant (C₁₂EO₂) and phospholipids (POPC). *Acta Phys. Polonica. A.* **91**: 953–960.
36. Yang, L., and H. W. Huang. 2002. Observation of a membrane fusion intermediate structure. *Science*. **297**: 1877–1879.
37. Funari, S. S., and G. Rapp. 1999. A continuous topological change during phase transitions in amphiphile/water systems. *Proc. Nat. Acad. Sci. USA.* **96**: 7756–7759.
38. O'Connor, L. J., T. Nicholas, and R. M. Levin. 1999. Subcellular distribution of free fatty acids, phospholipids, and endogenous lipase activity of rabbit urinary bladder smooth muscle and mucosa. *Adv. Exp. Med. Biol.* **462**: 265–273.
39. Haeffner, E. W., and O. S. Privett. 1975. Influence of dietary fatty acids on membrane properties and enzyme activities of liver mitochondria of normal and hypophysectomized rats. *Lipids*. **10**: 75–81.
40. Courtois, M., S. Khatami, E. Fantini, P. Athias, P. Mielle, and A. Grynberg. 1992. Polyunsaturated fatty acids in cultured cardiomyocytes: effect on physiology and beta-adrenoceptor function. *Am. J. Physiol.* **262**: H451–H456.
41. Lu, G., T. A. Morinelly, K. E. Meier, S. A. Rosenzweig, and B. M. Egan. 1996. Oleic acid-induced mitogenic signaling in vascular smooth muscle cells, a role for protein Kinase C. *Circ. Res.* **79**: 611–619.
42. Wilschut, J. 1990. Membrane fusion in lipid vesicle systems. In *Membrane Fusion*. J. Wilschut and D. Hoekstra, editors. Dekker, Groningen. 89–126.
43. Clandinin, M. T., M. Foot, and L. Robson. 1983. Plasma membrane: can its structure and function be modulated by dietary fat? *Comp. Biochem. Physiol. B.* **76**: 335–339.
44. Trichopoulou, A. 1995. Olive oil and breast cancer. *Cancer Causes Control.* **6**: 475–476.
45. Trichopoulou, A., and P. Lagiou. 1997. Worldwide patterns of dietary lipids intake and health implications. *Am. J. Clin. Nutr.* **66**: 961S–964S.
46. Tzounou, A., C-C. Hsieh, A. Polychronopoulou, G. Kaprinis, N. Toupadaki, A. Trichopoulou, A. Karakatsani, and D. Trichopoulos. 1993. Diet and ovarian cancer: A case-control study in Greece. *Int. J. Cancer.* **55**: 411–414.
47. Asano, M., K. Masuzawa, T. Matsuda, and T. Asano. 1988. Reduced function of the stimulatory GTP-binding protein in beta adrenoceptor-adenylate cyclase system of femoral arteries isolated from spontaneously hypertensive rats. *J. Pharmacol. Exp. Ther.* **246**: 709–718.
48. Keller, S. L., S. M. Bezrukov, S. M. Gruner, M. W. Tate, I. Vodyanov, and V. A. Parsegian. 1993. Probability of alamethicin conductance states varies with nonlamellar tendency of bilayer phospholipids. *Biophys. J.* **65**: 23–27.
49. Goldfine, M., J. J. Rosenthal, and N. C. Johnston. 1987. Lipid shape as a determinant of lipid composition in *Clostridium butyricum*. The effects of incorporation of various fatty acids on the ratios of major ether lipids. *Biochim. Biophys. Acta.* **904**: 283–289.
50. Cavagnetto, F., A. Relini, Z. Mirghani, A. Gliozzi, D. Bertoia, and A. Gambarcorta. 1992. Molecular packing parameters of bipolar lipids. *Biochim. Biophys. Acta.* **1106**: 273–281.
51. Kleinfeld, A. M. 1990. Lipid and protein structure of biological membranes. In *Membrane Fusion*. J. Wilschut, and D. Hoekstra, editors. Dekker, Groningen. 3–33.